Patrick Bürger (Autor)

High-Temperature Electrostatic Precipitation: Fundamentals, Phenomena and Feasibility

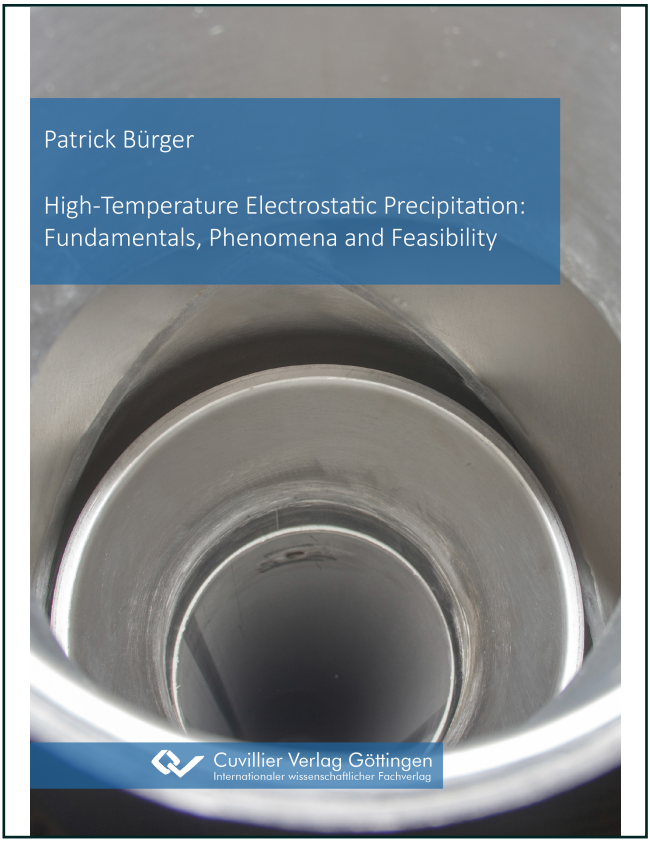

https://cuvillier.de/de/shop/publications/8865

1 Introduction

High temperatures are required in many industrial applications such as: glass furnaces and cement kilns; pyrolytic, metallurgical, and ceramic processes; waste incineration and fossil fuel combustion in power plants; and the flame-based production of functional (nano)particles. Therefore, a technology suitable for high-temperature (HT) gas cleaning (above 673 K or 400 °C) offers huge potential for the improvement of resource and heat recovery processes, the effective protection of catalyst beds and gas turbines, and the fractionated separation of particulate matter at different temperatures.

The high energy demand of HT processes requires the efficient use of (fossil) resources for ecological and economic reasons, especially under the consideration of the goals set in the Paris Climate Accords from 2015 and the more recent threat to the security of energy supplies in Europe due to the Russian invasion of Ukraine. To minimize energy demands, effective heat integration must be conducted throughout the HT processes and excess heat must be used sensibly in other applications. However, efficient heat recovery from dusty gases is not trivial due to the resulting particle deposition on heat exchanger surfaces. Meanwhile, the decarbonization of industrial processes by substituting fuels or entire processes is gaining traction in research and industry.

To achieve efficient heat recovery from hot gases, particulate matter must be separated beforehand. Above 673 K (400 °C), only two technologies are available which have considerable drawbacks depending on the designated application. Gas cyclones can be used up to very high temperatures, but they are not suitable for the removal of nanoparticles due to their typical cut size between 2 – 10 µm (Brauer 1996). Surface filtration with ceramic or sintered metal filter cartridges allows particle removal up to several hundred degrees Celsius but produces a very high pressure drop. Nanoparticle removal is even more challenging than the removal of larger particles, because the channels in the filter cake become much narrower increasing the pressure drop even further. Additionally, sintering processes may block parts of the filter area as nanoparticles show the tendency to sinter well below the sintering temperature of the bulk material (Zeng et al. 1998). Due to these difficulties, the hot gas is typically cooled down in industrial processes and particle separation is handled at a more convenient temperature, resulting in the loss of valuable high-caloric heat.

Therefore, the development of an energy efficient high-temperature gas cleaning technology suitable for any particle size could lead to a significant improvement in heat recovery in industrial processes. Since the 1960s, the concept of electrostatic precipitation has been investigated as an alternative for high-temperature gas cleaning. In many cases the measurements were conducted on a small lab-scale only and did not proceed to experiments assessing the capability for particle separation above 673 K. Additionally, the removal of nanoparticles and the relevant charging mechanisms at higher temperatures were hardly ever investigated in detail.

To close these research gaps, in this dissertation the operation of a pilot-scale electrostatic precipitator is investigated between ambient temperature and 1073 K (800 °C). This is to further the understanding of the fundamental processes of HT electrostatic precipitation and to ascertain the potential and feasibility of the technology at high temperatures.

2 Fundamentals of electrostatic precipitation

Electrostatic precipitation is a very robust and reliable technique for gas cleaning applications. In 1906, Frederick G. Cottrell started to apply his ground-breaking laboratory work on electrostatic precipitation in industrial applications with huge success. By 1911, the first large-scale industrial unit at a smelter was operable, cleaning over 400000 m^3/h of stack gas (White 1977). Electrostatic precipitators (ESPs) work over a wide range of operating pressures and temperatures and cause a low pressure drop. An ESP is capable of removing even nm-sized aerosols from gas streams with remarkable separation efficiency while maintaining a moderate energy demand. A well-designed ESP can operate flawlessly for many years. However, under some circumstances ESPs are difficult to design since the engineer must consider a variety of influences induced by, among others: pressure, temperature, gas composition, humidity, ESP configuration, electrode geometry, particle size, particle shape, particle concentration, state of particulate matter, dust resistivity and residence time. Extrapolating experience from another project may not suffice, and laboratory or pilot plant experiments are advisable to ensure the best performance of a new installation.

Despite these challenges, ESPs are widely used in various sectors of the industry. First and foremost, they are often used in the exhaust gas purification section of power plants burning fossil fuel or residual waste. Other common applications are the removal of liquid acids from gas streams in the chemical industry, precipitation of welding fumes and oil mists in the metalworking industry, exhaust gas purification in steel mills and cement plants, and as the particle removal concept in some air-conditioning applications. Additionally, ESPs are used in the production of goods to separate valuable components from gas streams (e.g. spray drying processes), for instance in the food industry (St. George and Feddes 1995) and the pharmaceutical industry (Raula et al. 2004; Dobrowolski et al. 2018). Due to their simple design, cleaning-in-place procedures can be applied easily which is very important for processes where following hygiene regulations is paramount. Additionally, ESPs may play an important role for the efficiency of additive manufacturing processes and upcoming pyrolytic processes. Even NASA is considering an ESP for its Mars mission to protect the chemical processes of the in-situ resource utilization unit from dust particles under the extreme conditions of the Martian atmosphere (Calle et al. 2013; Johansen et al. 2018).

In the following subchapters, the basic principles of electrostatic precipitation are outlined to facilitate the understanding of the phenomena, results and theories presented in this dissertation.

2.1 General working principle

ESPs use the concept of a direct current (DC) corona discharge which supplies positive ions or negative ions and free electrons, depending on the polarity at the discharge electrode. These charge carriers can charge the aerosol particles on impact which makes them susceptible to electric fields. The potential difference between the high voltage (HV) discharge electrode and a close-by grounded collection electrode results in an electric field providing the driving force for electrostatic

precipitation. Particles charged by charge carriers from the corona discharge migrate towards the collection electrode where they will be deposited and retained by electrostatic forces. Periodically, the growing dust layer on the collection electrode must be removed to maintain good separation efficiency. The removed dust is collected at the bottom of the housing and removed by appropriate equipment (e.g., rotary valve). Therefore, the particle removal process by electrostatic precipitation is divided into several steps, most of them happening simultaneously.

- Formation of charge carriers
- Particle charging
- Particle migration
- Particle deposition
- Dedusting and residue processing

Based on their design and operation mode, ESPs can be grouped in different categories. The geometric design of ESPs can be split into two major categories, wire-plate and wire-tube configuration (see Figure 1). The wire is supplied with a high DC voltage, and therefore acts as the discharge electrode. However, the geometry and shape of the discharge electrode can deviate strongly from a classic wire for constructive or operational reasons. The plate or tube, respectively, is grounded for safety reasons and acts as the collection or precipitation electrode. In wire-tube configuration the wire is positioned coaxially inside the tube, in wire-plate configuration a set of equally distanced wires is located on the centre line between two parallel plates. In general, wire-tube configurations are often used for small and medium volume flow rates while wire-plate configurations are used frequently for large scale gas cleaning processes. Scale-up is conducted by using multiple tubes or channels in parallel because the geometry and the residence time play an important role in the precipitation process. While wires often serve as a discharge electrode in research due to the facilitated applicability of theoretical models, in industrial setups the wire is often replaced by sturdy rods with spikes to increase durability. However, the curvature of the discharge electrode is of great importance for the onset voltage of the corona discharge, which is discussed in chapter 2.2.1.

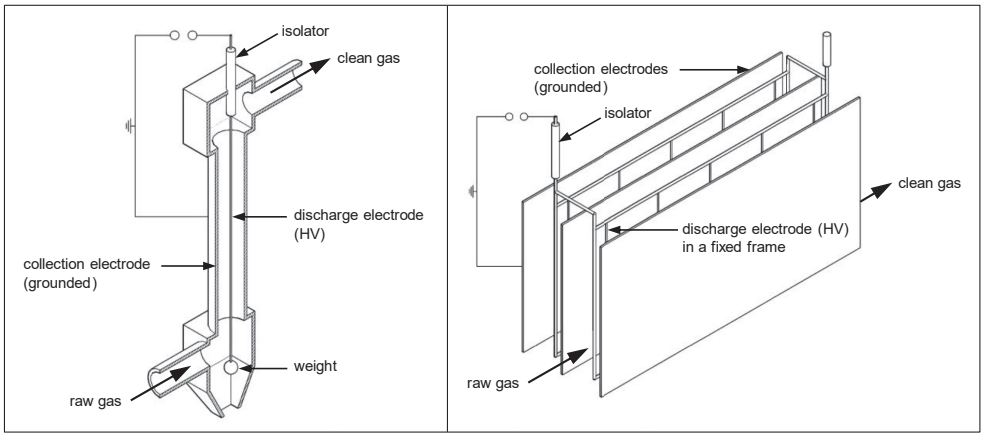

Figure 1: Schematic of typical ESP configurations: wire-tube ESP (left) and wire-plate ESP (right).

Another distinction of ESPs is their operation in dry or wet mode. ESPs operated in dry mode are very common and require periodic dedusting of the collection electrode to maintain good separation efficiency. The frequency strongly depends on the raw gas concentration and the properties of the precipitated particles. Depending on the construction type and process parameters, different dedusting methods can be applied. In many cases (especially for wire-plate ESPs), vibrations are applied to the collection electrode to remove the precipitated dust layer. The dust falls off and is subsequently collected and removed in the dust hopper. During this process, some re-entrainment will occur. This must be handled by another ESP segment in series which requires less frequent dedusting cycles due to the lower particle concentration. Alternatively, pulse jet dedusting can be used, especially for wire-tube configuration. Wet ESPs use a liquid film running down the collection electrode which captures the precipitated particles while simultaneously removing them from the collection electrode. Wet ESPs can maintain extremely high separation efficiencies because re-entrainment is not an issue. However, the liquid must be separated from the particles to be recycled and the wet particles must be processed further which increases overall costs.

Besides wet or dry mode, an ESP can be designed as a single stage or as a two-stage design, where the charging and collection process are separated. While the charging stage is basically a short ESP, the collection stage operates with strong electric fields but without a corona discharge by using a large diameter HV electrode. Therefore, the electric current in this stage is solely from the precipitation of charged particles. Two-stage designs may be advisable to maximize energy efficiency or when the dust properties require special treatment. However, some particles will be collected in the charging section which has to be dedusted on a less frequent schedule than the second stage. Additionally, re-entrainment of particles must be negligible (e.g., liquid aerosols or wet second stage) since in the collection stage these particles cannot be recharged and subsequently redeposited.

The operating voltage range of an ESP is described by the current-voltage characteristic, starting with the onset voltage U_0 and ending with the sparkover voltage U_{spark} as shown in Figure 2.

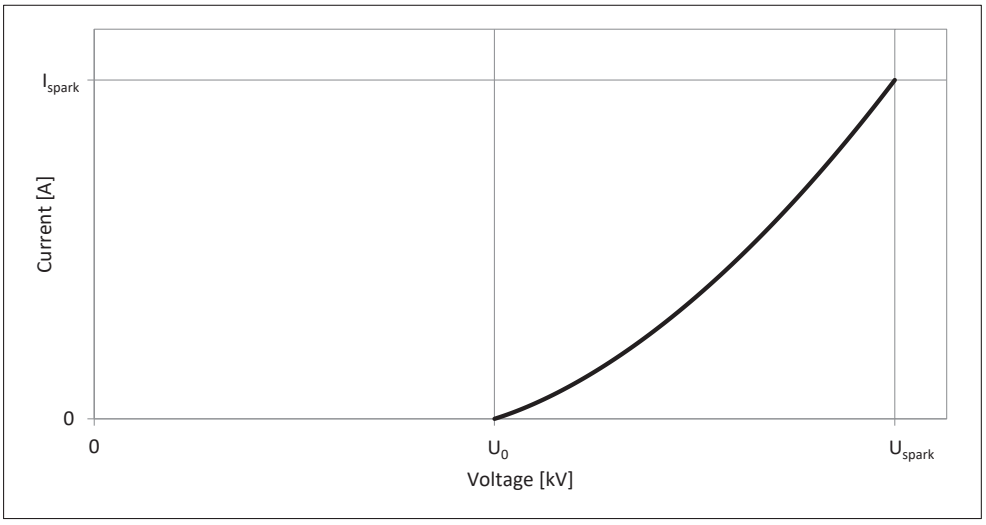

Figure 2: Schematic description of the ESP operating voltage range by the current-voltage characteristic.

Above the onset voltage, a progressive rise of the current is observed with an increase in operating voltage. Typically, ESPs are operated near the sparkover voltage to maximize the electric field. Thus, the HV power supply must be capable of providing sufficiently high currents and operating voltages. The actual values depend on the geometry of the ESP and the operating conditions such as pressure, temperature, gas composition and particle concentration.

The following chapters give an introduction to the corona discharge, the current-voltage characteristics, the particle charging process and particle migration in the electric field. Throughout this dissertation, mainly theoretical concepts valid for wire-tube geometry are explained and used. This is due to the applicability of analytical solutions and simplified equations, allowing an in-depth investigation of the phenomena associated with high-temperature electrostatic precipitation.

2.2 Corona discharge

The so-called corona discharge is a local self-sustaining gas discharge occurring under strong inhomogeneous electric fields when the electric field surpasses a certain threshold at the surface of the discharge electrode. The corona discharge causes gas ionization near the electrode surface which is called the active zone. The inhomogeneous field prevents a complete electrical breakdown of the inter-electrode gap. Gas ions leaving the active zone have the same polarity as the HV supplied to the discharge electrode. The following subchapters describe ESP related aspects of the corona discharge.

2.2.1 Onset criterion

The onset criterion of a corona discharge is the exceedance of a critical value for the electric field at the surface of the discharge electrode. Below this threshold, the gas discharge cannot sustain itself due to a lack of ionization events (Townsend and Edmunds 1914). Above this threshold, gas molecules are ionized close to the wire surface which is described as the active zone. While the mechanisms contributing to the build-up of an ion concentration are polarity-dependent (see chapter 2.2.2), the onset electric field E_0 is mainly influenced by gas composition, gas density, and curvature of the discharge electrode (Peek 1920; White 1963). The first comprehensive study on E_0 in wire-tube geometry was conducted by Peek (1915) where the influence of gas density, discharge electrode radius and geometry was investigated, among other issues. Based on the findings an empirical correlation was derived in that study valid for a wire radius r_w range of 10^{-4} – 10^{-2} m which is still in use over 100 years later. Two versions of the equation can be found in literature:

$$E_0 = 3.1 \cdot 10^6 \frac{V}{m} \delta_{gas} \left(1 + \frac{0.0308}{\sqrt{\delta_{gas}\, r_w\, 1m^{-1}}}\right) \; with \;\; \delta_{gas} = \frac{p}{p_{ref}} \frac{T_{ref}}{T} \tag{2-1}$$

with p_{ref} = 101325 Pa, T_{ref} = 298 K, valid for air (Peek 1915; from: Monrolin et al. 2018), and:

$$E_0 = A\, \delta_{gas} + B \sqrt{\frac{\delta_{gas}}{r_w}} \; with \;\; \delta_{gas} = \frac{p}{p_{ref}} \frac{T_{ref}}{T} \tag{2-2}$$

with p_{ref} = 101325 Pa, T_{ref} = 293 K, and A = 3.0·10^6 V/m and B = 9.0·10^4 V/m$^{0.5}$ (White 1963), or with p_{ref} = 101325 Pa, T_{ref} = 298 K, and A = 3.22·10^6 V/m and B = 8.46·10^4 V/ m$^{0.5}$ (Robinson 1971), valid for air. In these equations δ_{gas} is the relative gas density which relates the parameters to a specific reference temperature and pressure. A lower relative gas density leads to a reduction of E_0. In some versions of the Peek equation, the result is multiplied with a roughness factor f which is 1 for perfectly smooth wires and between 0.5 – 0.7 for well-used wires in the industry (White 1963).

Recently, Monrolin et al. (2018) derived an analytical solution for the positive corona onset field which is indeed a function of gas ionization properties and discharge electrode radius:

$$E_0 = \frac{E_{ief}}{\mathcal{W}_0\left(\frac{r_w\,\beta_{ef}}{ln(1+\gamma^{-1})}\right)} \qquad 2\text{-}3$$

where E_{ief} is the effective field required for ionization, $\mathcal{W}_0$ is the 0 branch of the Lambert $\mathcal{W}$ function, β_{ef} is a proportionality factor (based on gas composition) required for the calculation of the ionization coefficient α, and γ is the secondary electron emission coefficient. This equation allows for an accurate E_0 calculation for different gas compositions and for a wider range of r_w, especially below 10^{-4} m. However, obtaining values for the necessary parameters is not trivial in most cases.

The empirical correlation by Peek on the other hand is applied to both corona polarities (White 1963; Raizer 1991; Parker 1997) based on a negligible polarity difference for the onset fields. However, experimental data plotted on a logarithmic scale often reveal a well-defined onset voltage for positive corona, while negative corona shows a more gradual increase due to substantial sub-onset currents (Riebel et al. 2012). Therefore, the negative onset voltage cannot be pinpointed exactly.

Based on the assumption that the electric field is not altered by the low ionic space charge density just above corona onset, the onset voltage U_0 can be calculated from E_0 by:

$$U_0 = E_0\, r_w\, \ln\left(\frac{r_t}{r_w}\right) \qquad 2\text{-}4$$

for wire-tube geometry, where r_t is the collection electrode (tube) radius.

2.2.2 Polarity characteristics

Since research on corona discharges began, differences in the visual appearance and behaviour between positive and negative polarity were commonly observed (Paschen 1889; Watson 1910; Townsend and Edmunds 1914; Peek 1920). At voltages above the onset voltage but not close to sparkover, the positive corona discharge presents itself with a luminous violet glow covering the discharge electrode uniformly. The negative corona discharge can be identified by glowing violet spots placed irregularly on the discharge electrode. This can be observed when limiting the amount of ambient light and is caused by the emission of UV light during the ionization of the gas molecules. These early observations hinted towards underlying polarity dependent mechanisms for the corona discharge which can be grouped into two categories: the process of gas ion formation and the occurring microprocesses such as pulses and streamer.

For both polarities the inter-electrode gap of an ESP can be divided into two zones, the active zone (also called plasma zone) and the passive zone (or drift zone). By definition, the charge carriers in the passive zone are unipolar as the electric field is not strong enough to cause further impact ionization or plasma chemistry. This allows the unipolar charging of particles in the passive zone. The active zone around the discharge electrode is very thin compared to the passive zone and extends only about 2 – 10 electrode radii (depending on wire radius and discharge polarity) from the surface of the discharge electrode (Evans and Inculet 1978; Landers 1978; Chen and Davidson 2002).

Regardless of polarity, the corona discharge requires initial free electrons in the active zone to be triggered when the onset voltage is reached or surpassed. These are provided by ionization events from natural radioactivity or cosmic rays, which lead to the short-term formation of ion/electron pairs. In air at ambient pressure, about 10 – 20 pairs are generated per second and cm^3 (Broxon 1926; Loeb 1965). Without an electric field these pairs recombine quickly, but inside an electric field they are separated and attracted to the respective electrode of opposite polarity. Due to the strong electric field in the active zone, free electrons are accelerated and may obtain enough kinetic energy to cause impact ionization. The result of impact ionization is a positive gas ion and two electrons, one of them being the original electron. Based on this multiplication, the process is also called electron avalanche because each electron may cause more impact ionization events while in the active zone. The corona discharge must be sustained by the generation of new initial free electrons which can occur on several pathways besides the natural events stated above. Additionally, the corona discharge must be stabilized by the space charge of charge carriers in the passive zone in order to prevent a complete breakdown of the inter-electrode gap, also known as sparkover (White 1963).

Figure 3 visualizes the physical processes in a **positive corona discharge** in wire-tube geometry. The discharge electrode is on HV potential and the collection electrode is grounded for safety reasons.

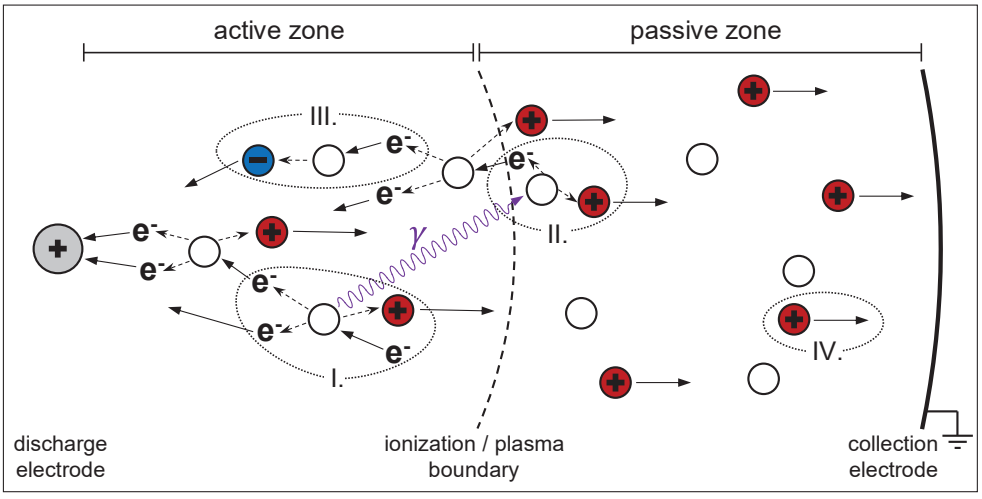

Figure 3: Visualization of the physical processes in a DC corona discharge with positive polarity (not to scale). (I.) Impact ionization of gas molecules, (II.) secondary electron emission by photo ionization of gas molecules, (III.) negative ion formation by electron attachment, (IV.) drift of positive gas ions in the unipolar passive zone.

Inside the active zone, free electrons are accelerated towards the discharge electrode and cause the impact ionization of gas molecules (I.) on their way. The produced positive gas ions leave the active zone driven by the electric field while the probability of recombination with an electron is negligible due to small recombination coefficients. Secondary electrons can be produced by the photo ionization of gas molecules (II.) which is caused by photon emission from the de-exciting species during impact ionization. Photo ionization can happen inside the active zone and at the edge of it. Free electrons can also attach to electronegative gas molecules (III.) on their way to the discharge electrode, forming negative gas ions in the process. This however is more likely at the outer parts of the active zone since the strong electric field near the discharge electrode accelerates the electrons sufficiently to favor impact ionization. At the ionization boundary, the rates for ionization and attachment are approximately equal. The current transport in the passive zone of positive corona discharges is governed only by positive gas ions drifting (IV.) towards the collection electrode. (White 1963; Robinson 1971; Chen and Davidson 2002; Monrolin et al. 2018)

The physical processes of the **negative corona discharge** are visualized in Figure 4 for the same geometry. Again, the discharge electrode is on HV potential and the collection electrode is grounded.

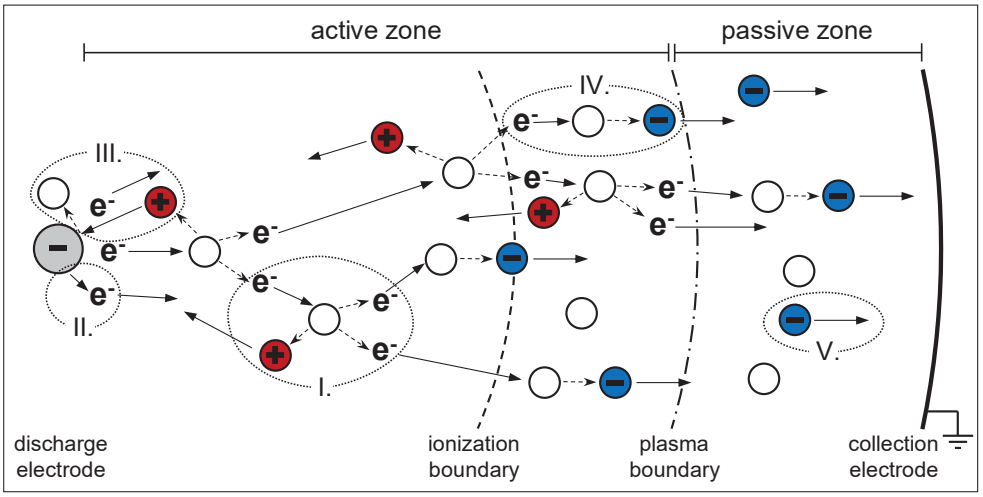

Figure 4: Visualization of the physical processes in a DC corona discharge with negative polarity (not to scale). (I.) Impact ionization of gas molecules, (II.) secondary electrons produced by photo emission from the discharge electrode, (III.) impact ionization on the discharge electrode surface, (IV.) negative ion formation by electron attachment, (V.) drift of negative gas ions in the unipolar passive zone.

In this case, the ionization boundary and the plasma boundary are not identical as the kinetic energy of many free electrons is still sufficient beyond the ionization boundary to cause impact ionization (Chen and Davidson 2003). Similarly to the positive polarity, the initial free electrons cause the impact ionization of gas molecules (I.). However, with negative polarity, the electrons travel towards the collection electrode and the positive ions drift towards the discharge electrode. Secondary electrons can be produced by either photo emission from the discharge electrode surface (II.), or to a lesser extent by the impact ionization of positive ions (III.) hitting the surface of the the discharge electrode. Inhomogenities on the wire surface tend to emit electrons which explains the visual

appearance of corona discharges with negative polarity. Beyond the ionization boundary, electron attachment onto electronegative gas molecules (IV.) is more likely than impact ionization. This allows the build-up of the space charge density required for stabilizing the corona discharge. In negative corona discharges, free electrons can provide a significant share of the current transport in the passive zone of a negative corona discharge together with the negative gas ions (V.) drifting towards the collection electrode. As more and more electrons attach to electonegative gas molecules, the electronic current contribution depends on the radius. (White 1963; Robinson 1971; Landers 1978; Chen and Davidson 2003)

The gas composition has a strong impact on the corona discharge for both polarities, but negative polarity requires the presence of a suffiecient content of electronegative gas molecules in order to build up the stabilizing space charge density in the passive zone and to prevent a sparkover near the onset voltage. Typical electronegative species are O_2, halogens or HX, H_2S and SO_2, however other species may facilitate the electron attachment process if present (White 1963; Robinson 1971). The details are discussed later in the context of possible influences on ESP operation (see chapter 3.2).

While these explanations on a microscopic level should suffice for the basic understanding of the charge carrier distribution in the inter-electrode gap required for the following chapters, in reality the corona discharge is far more complicated than this. Especially near the onset voltage and the sparkover voltage, underlying unsteady polarity-dependent microprocesses such as streamers and pulses have a significant impact on the behaviour of the corona discharge. For positive corona discharges, Burst-pulses, Geiger-pulses and pre-onset streamers are relevant microprocesses, whereas Trichel-pulses and streamers play an important role for negative corona discharges. A very detailed explanation of these processes can be found in the book on electrical coronas by Loeb (1965), in the German language in the doctoral thesis by Lübbert (2011), and in a more condensed form in other publications (White 1963; Robinson 1971; Chang et al. 1991; Morrow 1997).

2.2.3 Sparkover

While the onset voltage can be estimated theoretically as described above, the sparkover voltage is a mostly experimentally derived value as it depends on many variables and parameters. The sparkover event describes an electrical breakdown over the whole inter-electrode gap which establishes a conductive channel in the gas (arc discharge) consisting of gas ions and electrons. So-called pre-breakdown streamers are the mechanism behind this phenomenon. Inside the conductive channel the gas temperature is increased dramatically by the impact ionizations. (Loeb 1965; Raizer 1991; found in: Lübbert 2011; Lebedynskyy 2021)

The sparkover event leads to extremely high currents and the operating voltage drops to a few volts only while the arc discharge is active. Therefore, the corona discharge is extinguished resulting in a malfunction of the ESP for the duration of the spark. To protect the HV power supply, built-in control circuits lower the voltage when detecting a sharp rise in current. This stops the arc discharge until the HV cascade restores the previous voltage, yet again surpassing the sparkover voltage. To prevent excessive sparking, the operating voltage must be decreased below the sparkover voltage. Typically,

the sparkover frequency increases with operating voltage resulting in occasional arc discharges even below the sparkover voltage. In industrial applications a certain sparkover frequency is tolerated to obtain a higher operating voltage even though this means that the electric field vanishes for the duration of each sparkover event (White 1963).

According to the literature review by Lübbert (2011), many authors found that sparkover in air occurs at a mean electric field of 10 kV/cm in the inter-electrode gap with negative polarity and clean electrodes at standard temperature and pressure (STP). Throughout this dissertation STP refers to 293 K and 101325 Pa. For positive polarity under similar conditions, a value of 5 kV/cm is found. The higher operating voltage achievable with negative polarity is the main reason why industrial ESPs are operated with negative polarity in most cases.

Penney and Craig (1960) found that the dust layer resistivity strongly influences the polarity-dependent sparkover voltage and that the radius of the discharge electrode has an effect as well. Especially when highly resistive dust is covering the anode (discharge electrode for pos. polarity and collection electrode for neg. polarity) the sparkover voltage is reduced considerably. However, for thin wires (< 0.25 mm in diameter) a higher sparkover voltage was measured with positive polarity.

In general, one can assume that a mean electric field of 5 kV/cm is a good approximation for when to expect the sparkover voltage in wire-tube ESPs at STP while the geometry, the condition of the electrode surfaces and the aerosol play an important role (Lübbert 2011). The influence of temperature and pressure is discussed later (see chapter 3.2.3). A more detailed explanation of the sparkover mechanisms is given elsewhere (Loeb 1965; Raizer 1991).

2.3 Current-voltage characteristics

This chapter is based on published work by the author which discusses the measured current-voltage characteristics (CVCs) for this dissertation (Bürger and Riebel 2022b, CC BY 4.0 license).

"The CVC of corona discharges in wire-tube geometries was first described by Townsend. Implicitly, the derivation of the Townsend equation incorporates the following assumptions:

I. *Ions are emitted from the active zone only and hence are unipolar. The mobility of the gas ions is uniform and constant.*
II. *The field at the surface of the wire always is E_0, independently from the current density (Kaptzow´s hypothesis). The radial extension of the active zone and its effects on the overall potential distribution are negligible.*
III. *The transport of current outside the active corona zone is achieved by the drift of positive or negative gas ions, depending on the polarity of the corona wire. The corona current is limited by the ionic space charge. That is, the potential difference $\Delta U = U - U_0$ between the operation voltage U and the corona onset voltage U_0 is exactly equal to the potential difference produced by the space charge of the charge carriers in the inter-electrode gap.*

The Townsend equation exists in several variations (Townsend 1914; White 1963; Parker 1997) For wire-tube coronas, the most simplified version of the Townsend equation is written as: